2022 IEEE 2nd International Conference on Sustainable Energy and Future Electric Transportation (SeFeT) | 978-1-6654-8057-4/22/$31.00 ©2022 IEEE | DOI: 10.1109/SeFeT55524.2022.9909249

Performance Evaluation of Differential Mode Zeta Inverter using Various Modulation Schemes

Kartik Tank[1], Man-Mohan Garg[2], Nitin Gupta[3] and B L Narasimharaju[4]
[1,2,3]Department of Electrical Engineering, Malaviya National Institute of Technology Jaipur, India
[4]Department of Electrical Engineering, National Institute of Technology Warangal, India
Email: [1]kartik.tank96@gmail.com

***Abstract*— Conventionally, two stages are used for DC to AC voltage conversion. In the first stage, the boost converter provides voltage gain, and the H-bridge inverter provides the DC-AC conversion in the second stage. The two-stage conversion process can be reduced to a single-stage with the help of a new breed of inverter topology, namely differential mode inverter (DMI). For the same power rating, the single-stage DMI increases the energy density and compactness of the system compared to the two-stage. In DMI, using a specific DC-DC converter module, a higher voltage gain can be obtained. In this paper, a DC-DC Zeta converter based DMI is presented. The analysis of single-phase differential mode Zeta inverter (DMZI) is carried out with two different modulation schemes, namely Continuous mode modulation scheme (CMS) and Discontinuous mode modulation scheme (DMS). The steady-state analysis is performed to investigate the eight-order system. Generalized analytical expressions are derived, which are applicable to both modulation schemes. Also, a comparative analysis is presented to compare both modulation schemes by pointing out the requirement of maximum duty cycle, the voltage stress on the semiconductor switches, and system losses. Finally, MATLAB/SIMULINK results are provided to verify the analytical expressions.**

Keywords— Continuous mode modulation scheme, Differential mode inverter, Discontinues mode modulation scheme, Steady-state analysis, Voltage source inverter.

I. INTRODUCTION

Increment in power demand and depletion of non-renewable energy sources motivate the researchers to design compact and efficient power conversion systems. Moreover, a single-phase inverter is helpful for any islanded system. Conventionally, two stages are used for DC to AC voltage conversion. In the first stage, the boost converter provides voltage gain and the H-bridge inverter provides the DC-AC conversion in the second stage. Nowadays, differential mode inverter (DMI) is gaining popularity due to its compact design for low-power applications. DMI topology can provide the bipolar voltage to the load. Moreover, the use of a specific DC-DC converter module (like boost converter, buck-boost converter, Cuk converter, zeta converter, etc.) in DMI can provide a higher voltage gain. Overall, the DMI can convert the two-stage conversion into a single-stage. Single-phase DMI uses two identical DC-DC converters (or three in a three-phase inverter). Each DC-DC converter can be called a "Module". All modules have two-quadrant operation capability with bidirectional current (or power) flowability. In DMI topology, the input terminal of each module is parallelly connected with the same DC source, and load is connected between both module's positive output terminals, as shown in Fig. 1. The use of a similar module in DMI gives additional features such as scalability, modularity, etc. The use of a simple DC-DC converter is also a striking feature of DMI that resolves the problem of the maximum unity gain capability of traditional VSI. The output terminal of DMI can be connected with the AC grid having input renewable energy sources (like solar-panel, wind-mill etc.) that can contribute AC power to the grid. Similarly, a battery storage system (like electric vehicles and charging stations) can be charged at the input side in a differential mode rectifier (DMR) at grid-connected mode[1]-[2].

Slick use of particular modules with efficient modulation schemes can improve the performance of DMI [3]. Ref. [4] presents the boost converter based DMI. The use of a differential mode boost inverter is unable to ensure the soft starting of load. The buck-boost based DMI cannot provide ripple-free output current due to the absence of an output inductor [5]. [6] Cuk-based DMI is a strong candidate for DMI. However, it has inverting gain. Inverting gain of Cuk converter requires more circuitry to sense negative output voltage, which is a cause of slow output response of Cuk converter [7],[8].

Zeta converter belongs to the buck-boost converter family, which can increase or decrease the output voltage with respect to the input voltage. Zeta converter also has an output inductor that helps to soft start the load. However, the Zeta converter has the same number of components as the Cuk converter, but it has the non-inverting gain capability. Non-inverting gain capability makes the voltage sensing circuit simple and fast to respond the output voltage, compared to the Cuk converter [9]. Ref. [10] present differential mode zeta inverter (DMZI) with a continuous mode modulation scheme (CMS). The use of CMS for DMZI requires more output module voltage v_{o1} and v_{o2}. Conduction of both modules in a push-pull manner also increases the conduction and switching losses in the system. Whereas in a discontinuous mode modulation scheme (DMS), single module works at a time. Working of a single module in a complete load cycle reduces the conduction and switching losses compared to CMS. Also, DMS reduces the module output voltage level and voltage stress at the semiconductor switch compared to CMS. Lower voltage stress makes the system more cost-effective.

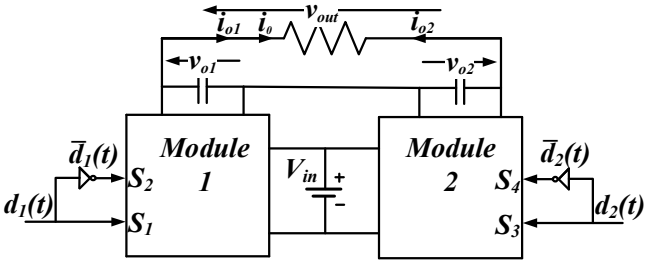

Fig. 1 Generalized circuit configuration of differential mode inverter

978-1-6654-8057- 4/22/$31.00 ©2022 IEEE

This paper is organized into five sections. Initially, Section II describes the steady-state analysis of DMZI and gives the generalized analytical formulas for inductor current and module voltage. Also, an analytical formula for load voltage is derived. Section III provides a detailed analysis of CMS and DMS. The variable duty cycle is derived to perform inverter operation in a particular modulation scheme. In section IV, a comparative analysis is given to indicate the superiority of DMS over CMS by comparing the requirement of maximum duty cycle, the voltage stress on semiconductor switches, and various losses in the inverter. The MATLAB/SIMULINK results verify the analytical expression. Finally, section V concludes the paper.

II. Analysis of Differential Mode Zeta Inverter

A differential mode zeta inverter is shown in Fig. 2, having two identical modules and sharing the same DC input voltage source. Load is differentially connected between the positive terminal of both modules. In DMZI, each module contains two bidirectional switches (main switch and synchronous switch). Each DC-DC converter requires a gate pulse of the desired duty cycle (or) to operate the switch. Here, the variable duty cycle d_1 refers to main switch S_1 of the first module, and duty cycle d_2 refers to main switch S_3 of the second module. Synchronous switches (S_2 and S_4) in each module are complementary to the main switches regardless of the modulation scheme i.e. $S_2 = \overline{S_1}$, and $S_4 = \overline{S_3}$. Comparison of variable duty cycle (d_1, d_2) with the sawtooth carrier signal generates the gate signal for particular switches. The voltages v_{o1}, v_{o2}, and v_o show the instantaneous output voltage of the first module, an instantaneous output voltage of the second module, and the voltage across the differentially connected load, respectively. Moreover, i_{o1}, i_{o2}, and i_o show the output current of the first module, second module, and load current, respectively.

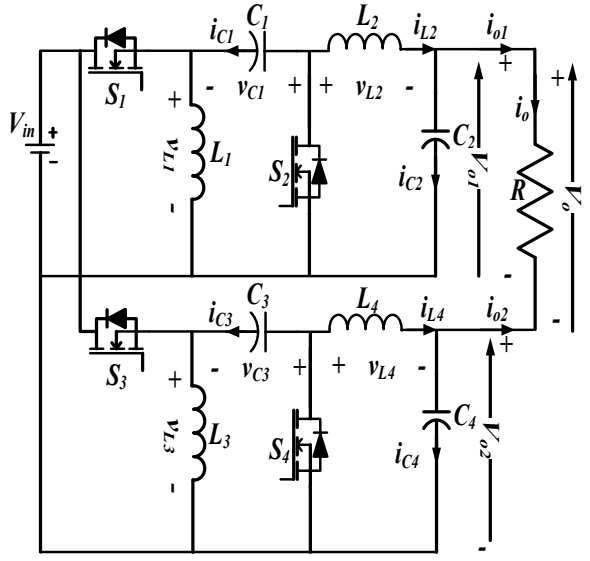

Fig. 2 Differential mode Zeta inverter Circuit

The analysis of a single inverter module is sufficient to evaluate the steady-state performance of the complete DMZI system. Fig. 3 shows the one module of a single-phase DMZI having two inductors L_1, L_2, and two capacitors C_1, C_2. The voltages v_{L1}, v_{L2} are the voltages across inductor L_1, L_2 and i_{C1}, i_{C2} are the currents through capacitors C_1, C_2 in module-1. Since both modules are identical in DMZI, similar notations are used for module-2 as module-1.

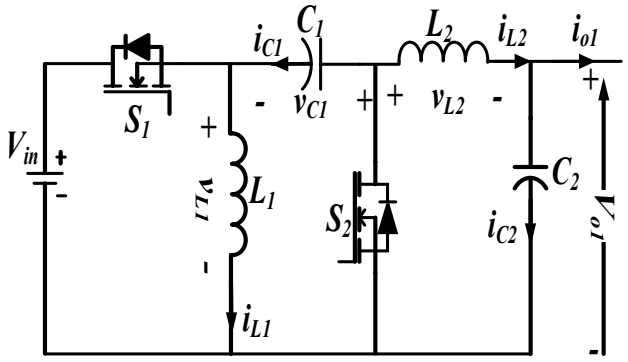

Fig. 3 Single module of DMZI

The modes of operation of the DMZI module are analyzed with the assumption that both the modules are working in continuous conduction mode (CCM). In CCM, DMZI has two operating modes in the positive load cycle as discussed below:

Mode-1 S_1 on, S_2 off (time interval $0 < t < d_1T_s$): In this mode, main switch S_1 is closed, and synchronous switch S_2 is open, as shown in Fig. 4(a). In this interval, inductors, L_1 and L_2 are charged by the input DC voltage source. Equations (1)-(5) show the relations after applying KVL and KCL at various loops and nodes.

$$v_{L1} = V_{in} \tag{1}$$
$$v_{L2} = V_{in} + v_{C1} - v_{o1} \tag{2}$$
$$i_{C1} = -i_{L2} \tag{3}$$
$$i_{C2} = i_{L2} - i_{o1} \tag{4}$$
$$v_{o1} = v_{C2} \tag{5}$$

Mode-2 S_1 off, S_2 on (time interval $d_1T_s < t < T_s$): In this mode, main switch S_1 is open, and synchronous switch S_2 is closed, as shown in Fig. 4(b). Inductor L_1 and L_2 are discharging. Equations (6)-(10) show the relations after applying KVL and KCL.

$$v_{L1} = -v_{C1} \tag{6}$$
$$v_{L2} = -v_{o1} \tag{7}$$
$$i_{C1} = i_{L1} \tag{8}$$
$$i_{C2} = i_{L2} - i_{o1} \tag{9}$$
$$v_{o1} = v_{C2} \tag{10}$$

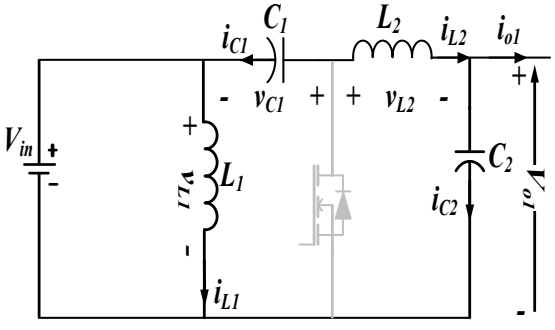

(a)

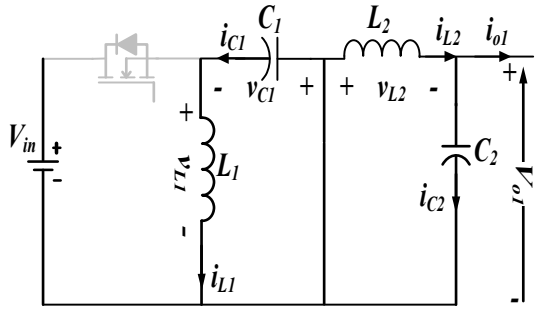

(b)

Fig. 4 Equivalent circuit of DMZI module (a) Mode-1 (b) Mode-2

The use of inductor volt-second balance and capacitor charge balance on (1)-(10) gives the steady-state module voltage (V_{o1}) and inductor currents (I_{L1}, I_{L2}) as follows [11].

$$V_{o1} = \frac{d_1}{d_1} V_{in} \tag{11}$$

$$I_{L1} = \frac{d_1}{d_1} I_{o1} \tag{12}$$

$$I_{L2} = I_{o1} \tag{13}$$

Similar to the first module, the second module of DMZI can be analyzed, which works with variable duty cycle d_2. Thus, replacing d_1 by d_2, V_{o1} by V_{o2}, I_{o1} by I_{o2}, and so on gives:

$$V_{o2} = \frac{d_2}{d_2} V_{in} \tag{14}$$

$$I_{L3} = \frac{d_2}{d_2} I_{o2} \tag{15}$$

$$I_{L4} = I_{o2} \tag{16}$$

Fig. 2 shows that the output current of the first module is the same as the output load current. Moreover, the output current of the second module is opposite to the load current, represented as (17).

$$i_{o1} = -i_{o2} = i_o \tag{17}$$

Due to the differential connection of load, the load voltage is given as (18). By using (11), (14) and (17), the average load output voltage can be derived as (19). Also, by using the mathematical expression, a voltage gain versus duty cycle curve is sketched in Fig. 5. Fig. 5(a) shows the unipolar gain curve for module-1. Similarly, Fig. 5(b) shows the unipolar gain curve for module-2. Fig. 5(c) shows the inverter output voltage across the load, which is bipolar in nature. Equations (20)-(23) are derived using (11)-(17), which further gives the genialized analytical expression for all inductors currents. All the analytical expressions are valid for both modulation schemes after substituting the relationship between the duty cycle d_1 and d_2.

$$v_o = v_{o1} - v_{o2} \tag{18}$$

$$V_o = \frac{d_1 - d_2}{(1-d_1)(1-d_2)} V_{in} \tag{19}$$

$$I_{L1} = \frac{d_1 (d_1 - d_2) V_{in}}{(1-d_1)^2 (1-d_2) R} \tag{20}$$

$$I_{L2} = \frac{(d_1 - d_2) V_{in}}{(1-d_1)(1-d_2) R} \tag{21}$$

$$I_{L3} = \frac{d_2 (d_2 - d_1) V_{in}}{(1-d_1)(1-d_2)^2 R} \tag{22}$$

$$I_{L4} = \frac{(d_2 - d_1) V_{in}}{(1-d_1)(1-d_2) R} \tag{23}$$

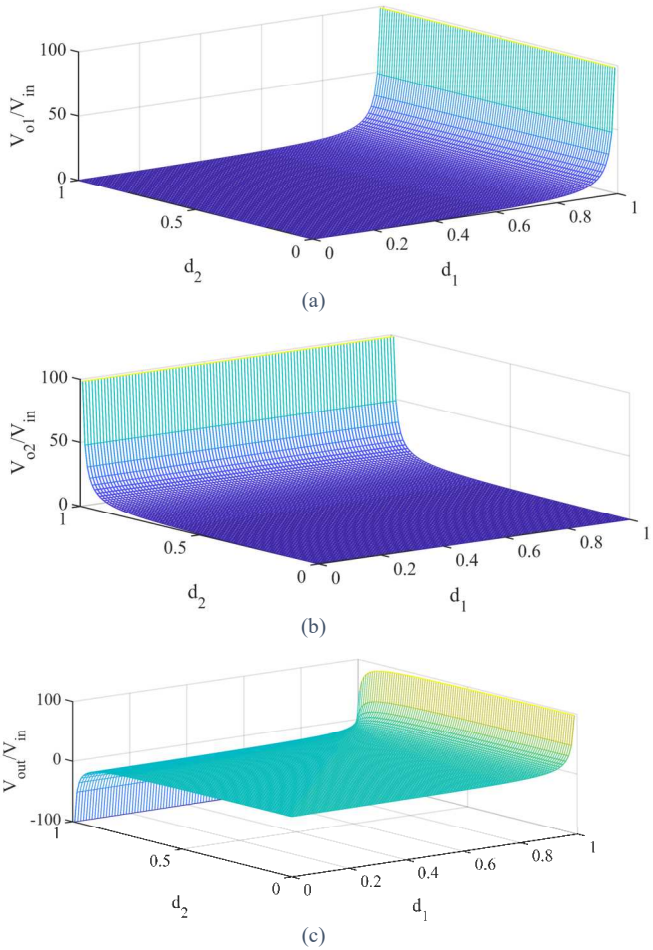

Fig. 5 Duty ration v/s gain curve for (a) Module-1 (b) Module-2 (c) DMZI

III. Modulation Schmeme for DMZI

Modulation schemes play a significant role in any inverter. Mainly DMI can work with two modulation schemes, namely, CMS and DMS. CMS is the most straightforward modulation scheme for single-stage DC-AC conversion. In CMS, both modules are operated with a complementary duty cycle i.e., $d_2 = \overline{d_1}$. References [12]-[13] provide more detail on CMS for the boost and Cuk-based DMI in which both the modules are working continuously. So, if $d_1=d$, then $d_2=1-d$ (since $d_2 = \overline{d_1}$). It indicates that a single gate signal can operate the complete inverter system. In this scheme, S_1, S_4 are operated with duty cycle d and S_2, S_3 with $(1-d)$.

Using (11), (14) and (18), the average load voltage (V_o) and duty cycle expression for CMS are obtained as given in (24) and (25), respectively.

$$V_o = \frac{2d-1}{d(1-d)} V_{in} \tag{24}$$

$$d = \frac{\left(\frac{V_m}{V_i}\right) sin(\omega t) - 2 + \sqrt{4 + \left(\frac{V_m}{V_i} sin(\omega t)\right)^2}}{2\frac{V_m}{V_i} sin(\omega t)} \tag{25}$$

In DMS [14]-[15], only a single module is working at a time. The first module works for the first half cycle of load voltage, and the second module is not operated. In the second half cycle of load voltage, the first module is not operated and the second module is working. Each non-operating module provides a return path for the load current. The variable duty cycles (d_1, d_2) for both modules are given in (26).

$$d_1 = \begin{cases} \dfrac{V_m \, sin(\omega t)}{V_m \, sin(\omega t) + V_{in}} & , v_o > 0 \\ 0 & , v_o \le 0 \end{cases}$$

$$d_2 = \begin{cases} 0 & , v_o \ge 0 \\ \dfrac{V_m \, sin(\omega t + \pi)}{V_m \, sin(\omega t + \pi) + V_{in}} & , v_o < 0 \end{cases} \tag{26}$$

Fig. 6(a) and Fig. 6(b) represent the critical waveform of duty cycles d_1 and d_2 for CMS and DMS, respectively. In DMS, zero duty cycle indicates no switching and conduction action in switch S_1 (in positive load voltage cycle) and S_3 (in negative load voltage cycle).

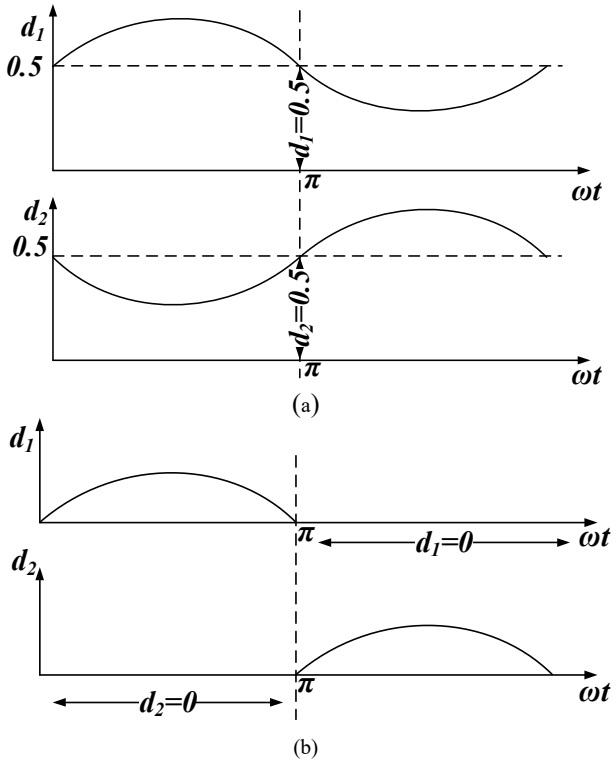

Fig. 6 Critical waveform of duty cycle for (a) CMS, (b) DMS

After putting duty cycles (d_1 and d_2) for CMS and DMS in (19)-(23), Table 1 indicates the various voltages and current expressions for CMS and DMS in the positive cycle of load voltage.

Table 1 Analytical Expressions for various currents and voltages for CMS and DMS

CMS	DMS
$V_{o1} = \frac{d_1}{1-d_1} V_{in}$	$V_{o1} = \frac{d_1}{1-d_1} V_{in}$
$V_{o2} = \frac{1-d_1}{d_1} V_{in}$	$V_{o2} = 0$
$I_{L1} = \frac{(2d_1-1)V_{in}}{(1-d_1)^2 R}$	$I_{L1} = \frac{d_1^2 V_{in}}{(1-d_1)^2 R}$
$I_{L2} = \frac{(2d_1-1)V_{in}}{d_1(1-d_1)R}$	$I_{L2} = \frac{d_1 V_{in}}{(1-d_1)R}$
$I_{L3} = \frac{-(2d_1-1)V_{in}}{d_1^2 R}$	$I_{L3} = 0$
$I_{L4} = \frac{-(2d_1-1)V_{in}}{d_1(1-d_1)R}$	$I_{L4} = \frac{-d_1 V_{in}}{(1-d_1)R}$
$V_o = \frac{2d_1-1}{d_1(1-d_1)} V_{in}$	$V_o = \frac{d_1}{1-d_1} V_{in}$

IV. Simulation Results with Comparative Analysis of CMS and DMS

A. Requirement of Maximum Duty Cycle: In order to obtain the same output voltage in both modulation schemes, (***25***) and (***26***) are simplified and the corresponding maximum duty cycle is obtained as follows:

$$\text{For, CMS} \quad d_{1,max} = \frac{k - 2 + \sqrt{4 + k^2}}{2k} \tag{27}$$

$$\text{For, DMS} \quad d_{1,max} = \frac{k}{k+1} \tag{28}$$

Here k is taken as $k = \frac{V_m}{V_{in}}$.

For the same load voltage, Fig. 7 indicates the ratio of the maximum required duty cycle value for CMS over DMS. A ratio $((d_{1\,CMS})_{max}/(d_{1\,DMS})_{max})$ higher than unity indicates that the requirement of duty cycle in CMS is higher than DMS.

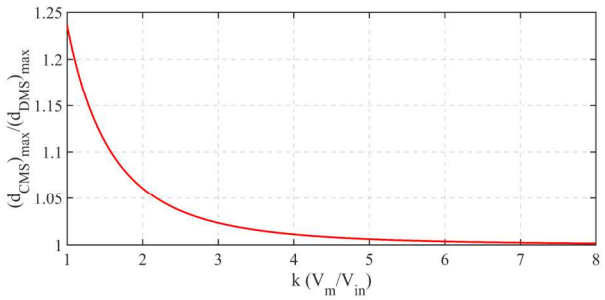

Fig. 7 Requirement of maximum duty cycle in CMS in comparison to DMS

B. Voltage stress on the switches: From Fig. 4, it can be analyzed that the peak inverse voltage (PIV) of switches is $V_{sw} = V_{o1} + V_{in}$. It implies that PIV depends on the module output voltage, given by (11) or (14). Since the $(d_{1\,CMS})_{max} > (d_{1\,DMS})_{max}$. This indicates that the switch PIV for CMS is greater than DMS.

Fig. 8(f) and Fig. 8(g) present the voltage stress across the switch in CMS. The ratings of all the switches are similar for CMS. In DMS, the switch rating is reasonably reduced, as

indicated in Table 2. Fig. 8(m) and Fig. 8(n) show the voltage stress along the switch S_1 and S_2, respectively. Similar voltage stress is obtained across the switch S_3 and S_4 with 180° shift to S_1 and S_2; therefore, they are not shown in the simulation results.

Table 2 Voltage stress across the switches in DMS

Load voltage cycle	Switch voltage stress
Positive half	$V_{S1} = V_{in} + V_m \sin(\omega t)$ $V_{S2} = V_{in} + V_m \sin(\omega t)$
Negative half	$V_{S1} = V_{in}$ $V_{S2} = 0$

C. Switching losses: Basically, three types of losses occur in power electronics converters. These are switching loss, forward conduction loss, and reverse blocking loss. In these three types of losses, switching loss is the major one compared to the forward conduction and reverse blocking loss. As explained in section III, In DMS, only a single module is operating for the complete load voltage cycle, which is two in CMS, as shown in Fig. 6. Conduction of a single module reduces the switching and conduction losses in DMS compared to CMS. The switch S_4 has no switching losses in positive output voltage from module perception in DMS, and S_3 is free from switching and conduction loss. Similarly, S_2 has no switching losses in negative output voltage, and S_1 is free from switching and conduction loss.

Specifications used for simulation are as follows: Output requirement: 50 Hz frequency 110 V (RMS) AC voltage using V_{in}=80 V. Parameter used for both modules: C_1=6.05 µF, C_2=10µF, L_1=L_2=0.57 mH, f_{sw}=25 kHz.

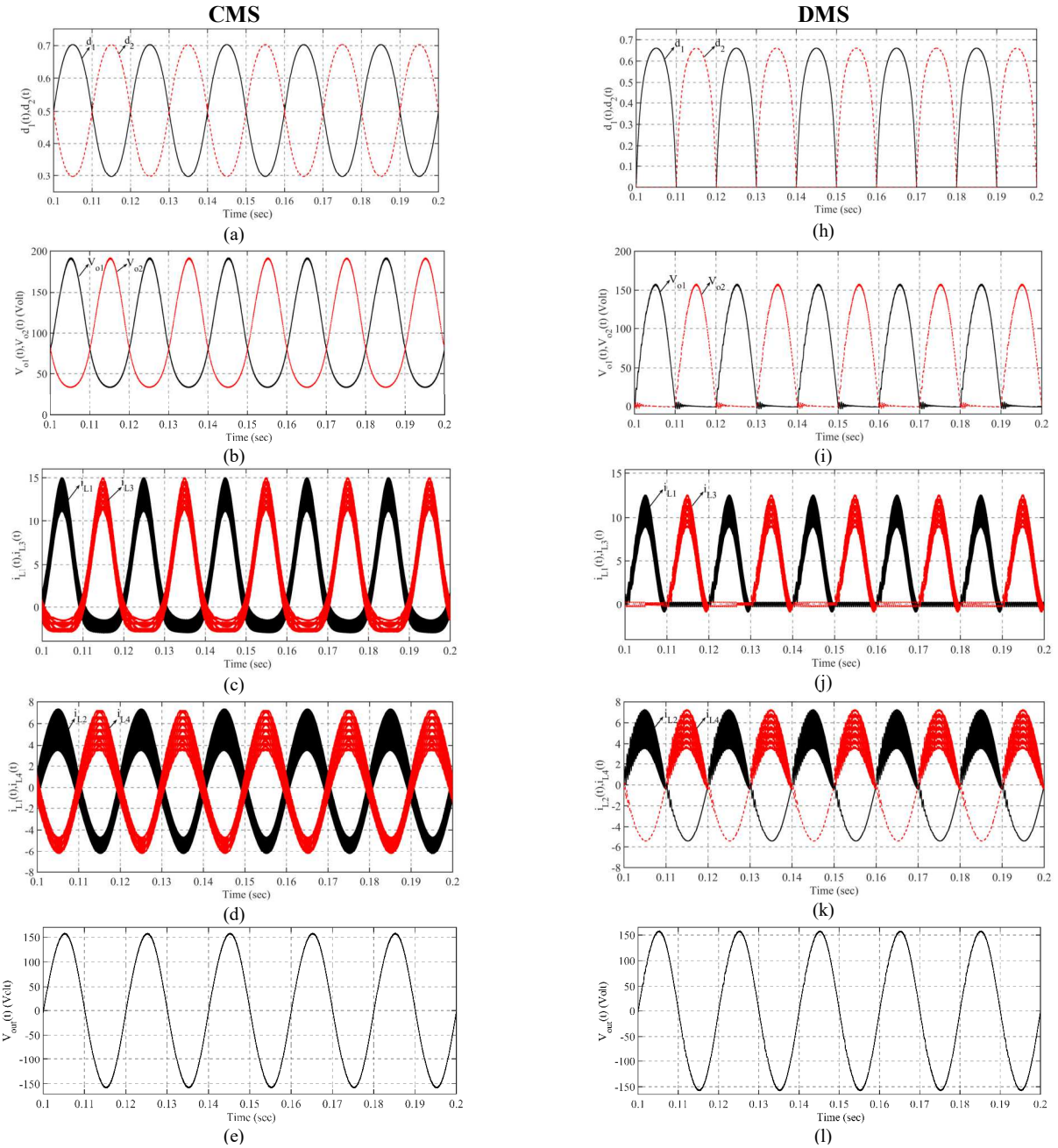

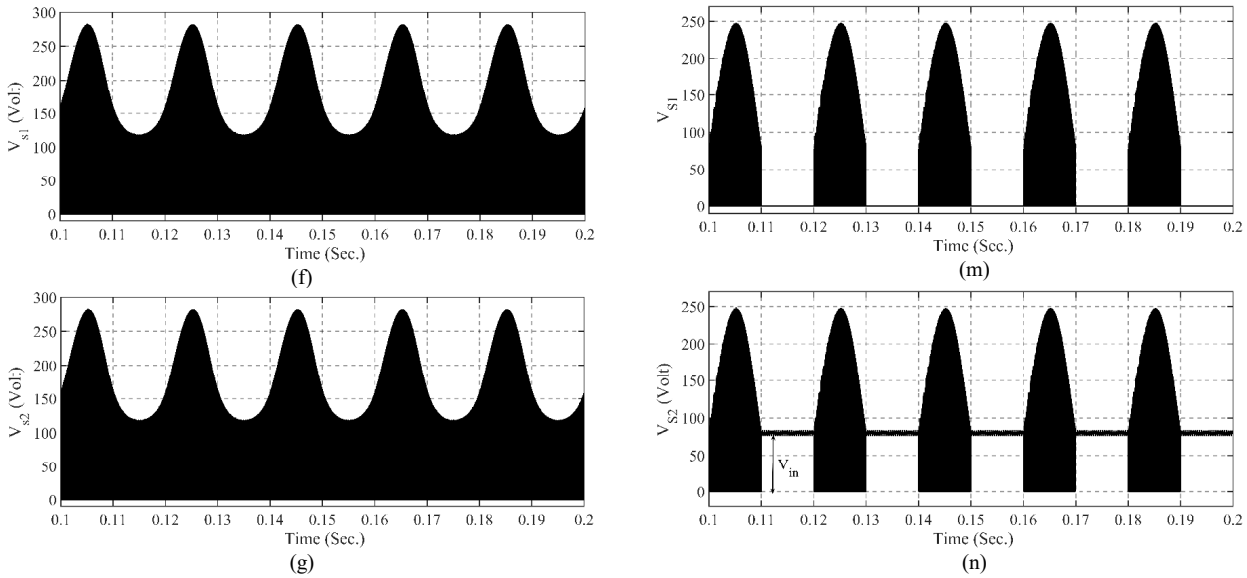

Fig. 8 Comparison between CMS and DMS-based DMZI:
Variable duty cycle, Module voltage, inductor current, load voltage, Switch voltage stress for (a)-(g) CMS, (h)-(n) DMS

As shown in Fig. 8, simulation results show that for the same load voltage, the requirement of maximum duty cycle in CMS is more than DMS, as shown in Fig. 8(a) and Fig. 8(h). The requirement of a higher duty cycle in CMS causes more module voltage and inductor currents in CMS as compared to DMS, as shown in Fig. 8(b)- Fig. 8(d) and Fig. 8(i)- Fig. 8(k). Since the switch voltage stress is dependent on module voltage, voltage stress in CMS is more than DMS, as shown in Fig. 8(f)- Fig. 8(g) and Fig. 8(m)- Fig. 8(n). The waveform of voltage stress across the switches also follows the expressions in Table *2* [refer Fig. 8(f)-Fig. 8(g) and Fig. 8(m)-Fig. 8(n)]. According to analytical expression, for the given value of parameters, the value of maximum required duty cycle ($(d_{1\,CMS})_{\max}$, $(d_{1\,DMS})_{\max}$), module voltage V_{o1} (or V_{o2}), inductor current I_{L1}, I_{L2}, I_{L3}, I_{L4} in positive load cycle, should be 0.703, 189 V, 12.78 A, 5.40 A, -2.28 A, -5.50 A respectively. However, the corresponding values for DMS are 0.661, 155.98 V, 10.54 A, 5.4 A, 0 A, and -5.41 A (in the same order as in CMS).

V. Conclusion

This paper analyzed the performance evaluation of a single-phase DMZI using two modulation schemes, CMS and DMS. Simulation results indicate that for obtaining the specified load voltage, the requirement of maximum duty cycle in DMS is less than CMS. This results in lesser module voltages, inductor currents, and switch voltage stress in the DMS. All analytical expressions followed the simulation results, as indicated by the simulation results. Also, the conduction of a single module in a particular load cycle reduces the conduction and switching losses in DMS. Thereby, DMS increases the efficiency and reduces the temperature of the device. Overall, the use of DMS along with DMZI makes the inverter efficient and power-dense.

References

1. N. Kumar, M. Mohmadi and S. Mazumder, "Experimental Validation of Single-Stage Three-Phase Non-Isolated Cuk Rectifier," 2019 IEEE Energy Conversion Congress and Exposition (ECCE), pp. 2744-2751, 2019.
2. M. Mohamadi, S. K. Mazumder and N. Kumar, "Integrated Magnetics Design for a Three-Phase Differential-Mode Rectifier," in IEEE Transactions on Power Electronics, vol. 36, no. 9, pp. 10561-10570, Sept. 2021.
3. Yaosuo Xue, Liuchen Chang, Sren Baekhj Kjaer, J. Bordonau and T. Shimizu, "Topologies of single-phase inverters for small distributed power generators: an overview," in IEEE Transactions on Power Electronics, vol. 19, no. 5, pp. 1305-1314, Sept. 2004.
4. Y. Tang, Y. Bai, J. Kan and F. Xu, "Improved Dual Boost Inverter with Half Cycle Modulation," in IEEE Transactions on Power Electronics, vol. 32, no. 10, pp. 7543-7552, Oct. 2017.
5. R. Kumar and B. Singh, "Buck–boost converter fed BLDC motor drive for solar PV array-based water pumping," in Proc. IEEE Int. Conf. Power Electron. Drives Energy Syst. (PEDES), pp. 1–6, Dec. 16–19, 2014
6. H. Soni, S. K. Mazumder, A. Gupta, D. Chatterjee and A. Kulkarni, "Control of Isolated Differential-Mode Single- and Three-Phase Ćuk Inverters at Module Level," in IEEE Transactions on Power Electronics, vol. 33, no. 10, pp. 8872-8886, Oct. 2018.
7. D. D. C. Lu and Q. N. Nguyen, "A photovoltaic panel emulator using a buck–boost dc/dc converter and a low-cost micro-controller," Solar Energy, vol. 86, no. 5, pp. 1477–1484, May 2012.
8. P. K. Singh, Y. V. Hote and M. M. Garg, "Comments on "PI and sliding mode control of a cuk converter"," in IEEE Transactions on Power Electronics, vol. 29, no. 3, pp. 1551-1552, March 2014,
9. R. Kumar and B. Singh, "BLDC Motor-Driven Solar PV Array-Fed Water Pumping System Employing Zeta Converter," in IEEE Transactions on Industry Applications, vol. 52, no. 3, pp. 2315-2322, May-June 2016.
10. K. K. H. Dia, M. A. Choudhury and Ahammad, "A single phase differential Zeta rectifier-inverter," 2015 IEEE International WIE Conference on Electrical and Computer Engineering (WIECON-ECE), pp. 284-288, 2015.
11. R. W. Erickson and D. Maksimović, Fundamentals of Power Electronics. Cham: Springer International Publishing, 2020.
12. R. O. Cáceres and I. Barbi, "A boost DC-AC converter: Analysis, design, and experimentation," IEEE Transactions on Power Electronics, vol. 14, no. 1, pp. 134–141, 1999.
13. S. K. Mazumder, R. K. Burra, R. Huang and V. Arguelles, "A low-cost single-stage isolated differential Cuk inverter for fuel-cell application," 2008 IEEE Power Electronics Specialists Conference, pp. 4426-4431, 2008.
14. C. Bao, S. Gupta and S. K. Mazumder, "Modeling and Analysis of Peak-Current-Controlled Differential Mode Ćuk Inverter," 2021 IEEE 12th International Symposium on Power Electronics for Distributed Generation Systems (PEDG), pp. 1-7, 2021.
15. S. Mehrnami, S. K. Mazumder and H. Soni, "Modulation Scheme for Three-Phase Differential-Mode Ćuk Inverter," in IEEE Transactions on Power Electronics, vol. 31, no. 3, pp. 2654-2668, March 2016.